Academic Journal of International University of Erbil

Journal Homepage: https://ojs.cihanrtv.com/index.php/public

PRINT-ISSN: 2519-6928

Online-ISSN: 3080-7174

Kinetic, isothermic, and thermodynamic investigations of the adsorption of metronidazole using a poly(3,4-ethylenedioxythiophene) adsorbent synthesized from deep eutectic solvent

Hana H. Abdulrahman [1], Hani K. Ismail [1]*

[1] Department of Chemistry, Faculty of Science and Health, Koya University, Koya 44023, Kurdistan Region – F.R., IRAQ

DOI: https://doi.org/10.63841/iue31636

Received 27 Jul 2025; Accepted 7 Aug 2025; Available online 22 Month 2026

ABSTRACT:

Oxaline, a deep eutectic solvent, was utilized for the inaugural synthesis of poly(3,4-ethylenedioxythiophene) (PEDOT) using chemical oxidation polymerization, which was used as an absorbent material for the adsorption of metronidazole (MET) from aqueous solutions. The formed adsorbent was characterized using a range of techniques, including Fourier transform infrared (FTIR) spectroscopy, Brunauer-Emmett-Teller (BET) analysis, scanning electron microscopy (SEM), energy-dispersive X-ray analysis (EDAX), and zeta potential methods. Additionally, adsorption tests were conducted to examine the impacts of MET concentration, pH, contact duration, and adsorbent dosage. The present results indicated a removal effectiveness of around 80.2% for MET under the following conditions: pH 6, 100 mg of adsorbent, a drug concentration of 100 mg/L, and shaking for 240 minutes. The adsorption process was thoroughly investigated using the kinetic and isothermal models. The Langmuir model and a pseudo-second-order kinetic model were found to be the best fits to the MET adsorption at 298 K. Additionally, the data demonstrated the high adsorption capacity of the PEDOT adsorbent at 86.80 mg/g for adsorption of MET. Analysis using thermodynamics showed that the adsorption process was endothermic and spontaneous. The adsorbent exhibited exceptional regenerative properties, allowing for reuse throughout five cycles. These findings underscore the efficacy of PEDOT as an absorbent for the efficient adsorption of MET from aqueous solutions.

Keywords: Conducting polymer, poly(3,4-ethylenedioxythiophene), deep eutectic solvents, adsorption, kinetic and isotherms, metronidazole.

1 INTRODUCTION

Over the years, there have been several synthetic substances created by humanity that could eventually affect and change the environment negatively [1]. As a result of the world economy's rapid growth, numerous inorganic (like metal and eutrophication ions) and organic (like dyes, pharmaceuticals, and surfactants) Pollutants have been discharged into the global aquatic ecosystem without adequate scientific cleanup [2, 3]. These pollutants' effects on human health and natural ecosystems are now a major concern [4]. Pharmaceuticals constitute significant aquatic organic pollutants, raising concerns over their environmental and health effects. The production and use of drugs have significantly increased in recent decades owing to substantial advancements in medicine. Approximately 3,000 chemicals are employed as pharmaceuticals, with hundreds of tons produced each year [5, 6]. The utilization of pharmaceuticals is associated with population growth, impacting both human and environmental health [7-9]. Among the most often used pharmaceuticals are analgesics, anti-inflammatory, and antibacterial pharmaceuticals [10]. These substances are added into municipal water and sewerage networks by pharmaceutical firms, medical facilities, and treatment plants [11]. Metronidazole is an antibiotic which is frequently employed in both human and veterinary medicine (see Figure 1 for its chemical structure) [12, 13].

*Corresponding author: hani.khalil@koyauniversity.org

Metronidazole (2-methyl-5-nitroimidazole-1-ethanol, MET) is a pale yellow, crystalline powder that tastes harsh and has a slight smell. It has a molecular weight of 171.12 g/mol and the chemical composition $C_6H_9N_3O_3$, making it one of the most widely used antibiotics in the world. This antibiotic, termed Flagyl, belongs to the nitroimidazole class and is utilized in the treatment of infectious diseases as an antimicrobial, antibacterial, and antiprotozoal agent. This cost-effective drug has been utilized for over 50 years in the treatment of amoebiasis, trichomoniasis, and anaerobic microbes, such as *Helicobacter pylori* and *Giardia lamblia*. It serves as an anti-parasitic component in poultry and aquaculture feeds [13-15]. This non-biodegradable, water-soluble substance (9.5 g L^{-1} at 25°C) may accumulate in aquatic environments due to its low *log* k ow (~ -0.1). Numerous studies have revealed the existence of 10–30 ng/L MET in water, with higher quantities seen in wastewater. The removal of MET from water is essential because to its toxicity, carcinogenic properties, and potential for inducing microbial resistance [16, 17]. Owing to their hydrophilic characteristics and restricted biodegradability, merely 20–50% of antibiotics may be digested in humans and animals, while the remainder is excreted. Residual drugs affect ecosystems by promoting the proliferation of antibiotic-resistant genes and bacteria. By 2050, antimicrobial resistance might incur costs of $100 trillion and lead to 10 million fatalities annually [18]. A variety of processes have been suggested for the removal of antibiotics from wastewater, involving physical-processes like adsorption, membrane filtration, and reverse osmosis; chemical techniques such as electrocoagulation; biological strategies; such as aerobic or anaerobic process [19, 20].

Researchers are particularly interested in the process of adsorption. This is due to its user-friendliness and other advantages. It functions effectively, is cost-efficient, and facilitates straightforward recovery and reutilization of the adsorbent. It is highly efficient in the large-scale removal of antibiotics [21, 22]. Various kinds of adsorbents have been investigated to remove organic pollutants from aqueous solution, including clay materials [23], carbon xerogels [24], functionalized biochar [25], metal oxide nanocomposites [26], chitosan [27], carbonaceous substances [28], zeolites [29], and mesoporous molecularly imprinted polymers [30]. The efficacy of an absorbent relies on its high capacity, non-toxicity, ability to absorb pollutants, simplicity of preparation, and recyclability [31].

Conductive polymers (CPs), for example, polythiophene (PTh), polyacetylene, poly(p-aminophenol), polypyrrole (PPy), poly(3,4-ethylenedioxythiophene), and polyaniline (PANI) along with its derivatives, have been extensively studied for their efficacy in removing various contaminants from contaminated water, attracting considerable academic interest [32-34]. Their unique qualities derive from the monomers availability, ease of synthesis, and low production costs, as well as applications in different fields such as extraction, restoring the environment, electromagnetic attenuation, and electrochemical processes [35-38]. CPs can be readily produced in both aqueous and nonaqueous (ionic liquids/DESs) conditions by chemical or electrochemical techniques. Inorganic acids, including nitric acid (HNO_3), chloric acid ($HClO_3$), sulfuric acid (H_2SO_4), and hydrochloric acid (HCl), have been utilized as dopants in the production of conducting polymers. Nonetheless, the application of CPs in aquatic environments with these acids presents multiple challenges. For example, they release hydrogen gas due to the application of potent, toxic inorganic doping acids; this leads to the embrittlement of polymers, diminished thermal stability, and associated risks, along with alterations in morphology [39, 40].

Deep eutectic solvents (DESs) can be used as an alternative to aqueous solutions that include no HCl, H_2SO_4, or other inorganic acids [15, 41]. DESs are innovative solvents that operate similarly to ionic liquids, having been identified by Abbott et al. in 2003 [42]. Their characteristics encompass low cost, simpler production compared to ionic liquids, lack of hazardous strong inorganic acids in aqueous solutions, high solute solubility, significant ionic conductivity, and non-toxicity [43, 44]. They comprise a eutectic mixture of a quaternary ammonium salt that acts as a hydrogen bond acceptor (HBA) with a hydrogen bond donor (HBD). HBD compounds possess a hydrogen atom bonded to a moderately electronegative atom such as fluorine, nitrogen, or oxygen, while HBA compounds exhibit a partial positive charge [45].

The efficacy of removal depends on various factors, involving the solute's morphology, charge, size, and hydrophobicity, together with the surface charge, pore size distribution, surface area, and oxygen concentration of the sorbent [46]. Numerous multifunctional polymer adsorbents, including Fe_3O_4-chitosan nano-adsorbent [47], polyaniline-polypyrrole (PPY-PANi) copolymer [14], polypyrrole [48], cellulose-chitosan composite [49], and conjugated microporous polymers [50], have been developed in this area for the adsorption of metronidazole compounds from wastewater.

In this study, poly(3,4-ethylenedioxythiophene) (PEDOT) prepared from Oxaline-deep eutectic solvents via a chemical polymerization procedure, employing ammonium persulfate (APS) as the initiator. Oxaline-DES, a eutectic composition of oxalic acid and choline chloride, provides an eco-friendly, low-toxicity substitute for traditional organic and ionic liquids. Moreover, polymers synthesized in Oxaline-DES exhibit distinctive morphologies, sustainability, and structural features, which likely impacted their utilization in the synthesis of PEDOT in the present investigation, as opposed to traditional aqueous-acid polymers. It also improves the stability and durability of the resulting polymer films at elevated temperatures (e.g., 25 °C and 50 °C). These specific behaviors can influence porosity, conductivity, and adsorption sites, hence affecting the adsorption efficacy of metronidazole. This study aims to utilize PEDOT as adsorbent for the removal of metronidazole from aqueous solutions. The advantage of employing this particular adsorbent originates from its monomer, 3,4-ethylenedioxythiophene, which has various functional groups—sulfur, oxygen, and π-conjugated systems—in its chemical composition. This property endows the adsorbent with a significantly greater quantity of

reactive groups in contrast to alternatives that may possess only individual functional groups, such as polypyrrole, polyaniline, and polythiophene. These functional groups can easily link with those present in the structures of many contaminants. The functionalization of poly(3,4-ethylenedioxythiophene) derived from deep eutectic solvents might improve the efficacy and adsorption capacity of the innovative adsorbent for the removal of pharmaceuticals from aqueous solutions. This improvement is due to the existence of many functional groups on its surface, such as π-electron systems, sulfur, and oxygen groups. This PEDOT modification from Oxaline-DES has not been used for drug removal before, and there is no data on it. The characterization of the PEDOT adsorbent has been measured by multiple approaches, including Fourier transform infrared (FTIR) spectroscopy, Brunauer-Emmett-Teller (BET) analysis, scanning electron microscopy (SEM), and energy-dispersive X-ray analysis (EDAX). The influence of specific physical parameters, such as solution pH, drug concentration, adsorbent dosage, contact duration, and temperature, on adsorption efficiency was also examined. The adsorption results were assessed using kinetic models, thermodynamic parameters, and isotherm processes.

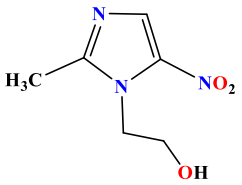

FIGURE 1 The chemical structures of metronidazole.

2 EXPERIMENTS

2.1 CHEMICALS AND REAGENTS

The purity of all the compounds used was analytical. All compounds used in the current study, namely, the 3,4-ethylenedioxythiophene (PEDOT) (Bidepharm, purity 99.99%), ammonium persulfate (APS, $(NH_4)_2S_2O_8$, Bio Chemo Pharma), oxalic acid ($C_2H_2O_4.2H_2O$, Sigma-Aldrich), choline chloride (Bidepharm, 97%), hydrochloric acid (HCl, Bio Chemo Pharma, 37%), hydrogen peroxide (H_2O_2, Sigma-Aldrich), methanol and ethanol (extra pure 99.9%, Fisher), and sodium hydroxide (NaOH, Carlo-Erba) were utilized as obtained without additional purification.

2.2 PREPARATION OF DEEP EUTECTIC SOLVENT (DES)

In our study, the DES, oxaline, was synthesized by combining choline chloride (ChCl) and oxalic acid (Oxa) in a 1:1 molar ratio, followed by heating at 60°C in an oven for 1 h. Next, we stirred the solution on the magnetic hotplate at 60°C for an additional 2 h until a clear homogenous solution was obtained, in accord with previous studies [51, 52].

2.3 SYNTHESIS OF POLY(3,4-ETHYLENEDIOXYTHIOPHENE) (PEDOT)

PEDOT was manufactured using chemical polymerization, as similar strategy to previous work [53, 54], utilizing 2.5 g of 3,4-ethylenedioxythiophene (EDOT) monomer mixed in 30 mL of oxaline-DES solvent, followed by stirring for 30 minutes, referred to as (solution 1). The prepared oxidant solution of ammonium persulfate (APS) served as the initiator by dissolving 4 g of it in 25 mL oxaline-DES as a dopant, resulting in solution 2. Subsequently, solution 2 was placed into a separating funnel to introduce the initiator to the monomers in solution 1 dropwise over the course of 2 h, while continuously stirring at room temperature (maintained at 25 °C,) to initiate the polymerization of the monomer. Upon completion of the dropwise addition, approximately 2 mL of H_2O_2 was added in several stages to augment the polymerization process. Upon concluding 8 hours of polymerization with stirring, allow the solution to rest overnight. Subsequently, the product was subjected to filtration, followed by a deionized water wash until a clean effluent was obtained. The wet polymer output was then processed in an oven at 70°C for 4 to 5 hours to produce dry polymer powder. **Fig. 2** depicts the suggested structure and reaction mechanism for the synthesis of PEDOT.

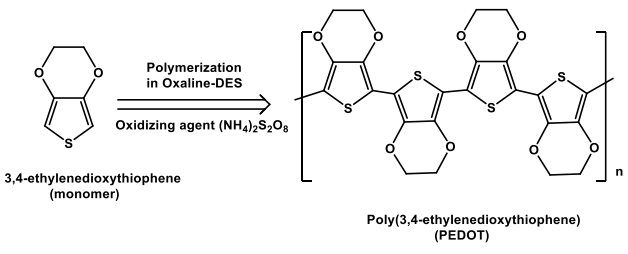

A)

FIGURE 2 In-situ oxidative polymerization process for synthesis of PEDOT.

2.4 PREPARATION OF MET PHARMACEUTICAL STOCK SOLUTIONS

To make a stock solution 500 mg/L, pure MET powder was separately dissolved in deionized water (DW) containing 10% absolute methanol (to fully dissolve the pharmaceutical). The quantity of MET required was calculated based on its molecular mass.

2.5 PH POINT ZERO CHARGE (PH_{PZC})

The pH at point of zero charge (pH_{pzc}) for the PEDOT was determined by adding 40 mg of material to solutions that had an initial pH of 2 to 10 (adjusted with 0.1 M NaOH and HCl solutions). The final pH was measured after 24 h of equilibrium at 298 K. The variation in pH during equilibration, ΔpH (the pH difference between the beginning and final values), was subsequently plotted against the original pH. The pH_{pzc} was ascertained according to the intersection of the initial and final pH values [55]. This procedure was executed in duplicate.

2.6 ADSORPTION STUDY

The experiments for adsorption were carried out at room temperature, with a pH meter (Adwa (AD8000)) to adjust the solution's pH using 0.1 M solutions of HCl and NaOH. A shaker (GFL Shaking Incubator 3031) was used to mix the samples with a precise amount of the adsorbent at 200 rpm for a predetermined amount of time in each experiment. The influence of several parameters was subsequently examined, including pH (2-10), adsorbent dosage (20 to 140 mg), initial concentration of pharmaceutical pollutant (20–200 mg/L), time of reaction (10–300 min), and temperature (298-313 K). The concentrations of MET were individually quantified prior and subsequent to adsorption by the adsorbent utilizing a UV/Vis Spectrometer (Alegent cary series 100 uv-vis spectrometer) at wavelengths of 320 nm for MET [13, 48]. The equilibrium adsorption capacity (q_e) and pharmaceutical adsorption percentage (*Removal* %) (equations 1-2) of the synthesized adsorbent were analyzed.

$$Removal\ \% = \frac{(C_i - C_e)}{C_i} \times 100 \quad (1)$$

$$q_e = \frac{(C_i - C_e)V}{M} \quad (2)$$

C_i is the initial concentration of the drug at time 0, C_e is the equilibrium concentration in mg/L, V is the volume of the drug solution in liters (L), and M is the mass of the adsorbent nanocomposites in grams (g). Furthermore, the mean adsorption from three measurements and the relative errors of the experimental findings were below 5%.

2.7 ADSORPTION MODELLING STUDIES

Kinetic adsorption tests were performed for 10 to 300 mins using water solutions of 100 mg/L of MET. The pH was set to its optimum, with other conditions reported in the figure captions. The kinetic models chosen for plotting the experimental data include pseudo-first-order, pseudo-second-order, and Elovich. Isothermal tests were conducted with increasing MET concentrations (20 to 200 mg/L) at the optimal pH and contact duration. The isotherm models (Temkin, Freundlich, and Langmuir) were used to create the isotherms using the experimental data's linear regression. The residual MET the solution was quantified via UV spectroscopy.

2.8 REGENERATION OF PEDOT ADSORBENT

To perform the adsorption-desorption studies, 100 mg of the adsorbent was introduced into 100 mL of MET solution (100 mg/L) in a conical flask with a stopper. The mixture was subsequently agitated for 240 min for MET. Thereafter, the adsorbent was centrifuged, and equation 1 was used to find the adsorption percentage. For the desorption process, 50 mL of methanol was mixed with the same adsorbent-loaded MET. The adsorbent was retrieved through centrifugation and reused for adsorption. To guarantee positive and repeatable outcomes, this process was carried out three times. UV-Vis spectrometry was employed to examine the supernatant solution. The desorption percentage was computed using equation 3.

$$Desorption\ \% = \frac{Amount\ of\ drug\ desorbed}{Amount\ of\ drug\ adsorbed} \times 100 \quad (3)$$

2.9 INSTRUMENTAL

A variety of techniques were utilized for the characterization and analysis of the PEDOT adsorbent. FTIR spectra were obtained using an FTIR spectrophotometer (Bruker, VBCTOR 22, USA) via the KBr-disc method as the background medium. The PEDOT composite's functional groups were identified by acquiring FTIR spectra across a wavenumber range of 400–4000 cm^{-1}. The Brunauer–Emmett–Teller (BET) using nitrogen adsorption-desorption isotherms within the P/P0 range of 0-1 and pore size distributions from 1 to 100 nm, was used to evaluate the surface area, and pore diameter distribution. At an accelerator voltage of 10 keV, scanning electron microscopy (SEM) (FESEM-TSCAN) was used to analyze the surface morphology. The elements included in the deposited polymer composite were characterized using

energy dispersive X-ray (EDX) spectroscopy.

3 RESULTS AND DISCUSSION

3.1 CHARACTERIZATION OF POLYMERIC SAMPLES

FTIR was employed to ascertain the presence of functional groups, elucidate chemical composition, and characterize molecular bonds within the substance. The FTIR study of PEDOT depicted in **Fig. 3A** exhibited several distinctive peaks as follows: The hydroxyl group in PEDOT's stretching vibration may be caused by the absorbed solvent is responsible for the broad band at 3435 cm^{-1}. Traces of the solvent (such as water, alcohol, or deep eutectic solvents) may still be present if the sample was not completely dried. The presence of the methylene (-CH_2) stretching mode is ascribed to minor peaks observed in the region of 2857–2923 cm^{-1}. The peak at 1714 cm^{-1} corresponds to the symmetric stretch of C-C=C, whilst the band at 1639 cm^{-1} is linked to -OH bending. The quinoidal structure of the thiophene ring is stretched C=C, while the thiophene ring is stretched C-C, as indicated by the peaks at 1490 cm^{-1} and 1351 cm^{-1}, respectively, showed the formation of PEDOT. The symmetrical and asymmetrical stretching of the ethylene dioxy group C-O-C generates the vibrational bands at 1226 cm^{-1} and 1071 cm^{-1}. The peaks at 982 cm^{-1} and 841 cm^{-1} are indicative of C–S stretching within the thiophene ring. The C-H bending vibration in the alkene moiety of the thiophene ring accounts for the peak at 921 cm^{-1}. A peak around 694 cm^{-1} may indicate the presence of a C–Cl bond originating from DES components such as choline chloride. The identified peaks correspond with the existing literature on the chemical polymerization of PEDOT [56, 57].

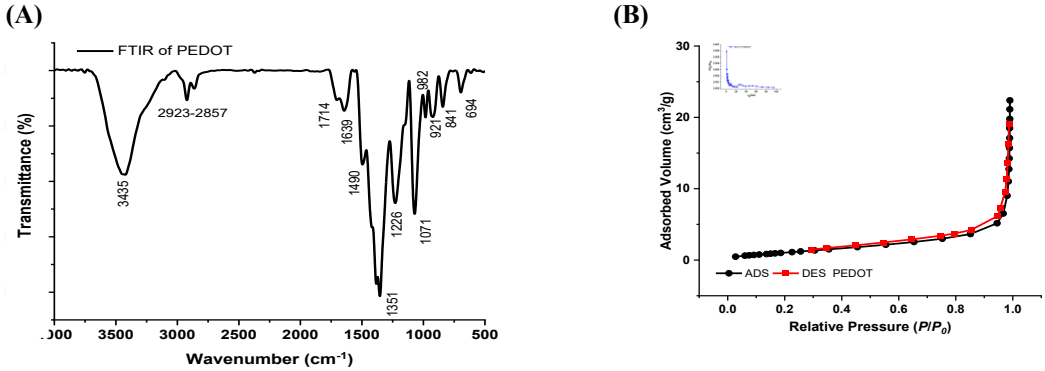

FIGURE 3 **(A)** FTIR spectrum of PEDOT. **(B)** Nitrogen adsorption–desorption isotherm of PEDOT and inset of figure 3B) is distribution of pore sizes for PEDOT.

The BET and BJH methods were employed to ascertain the specific surface areas and porosity characteristics of the materials by nitrogen adsorption–desorption isotherms, as seen in **Fig. 3B**. The hysteresis loop for PEDOT at relative pressures (P/P_o) was approximately 0.96. This outcome indicates that the PEDOT sample possesses a mesoporous structure. It was discovered that PEDOT had a mean pore diameter of 16.40 nm, a specific surface area of 21.65 m^2/g, and a total pore volume of 0.059 cm^3/g. Materials with pores less than 2 nm are considered microporous, those with sizes between 2 and 50 nm are mesoporous, and those with pores larger than 50 nm are macroporous [58]. The BJH plot (insert of **Fig. 3B**) indicates that the polymer pore size distribution ranged from 1 to 100 nm. This indicates the existence of two pore categories: (i) mesopores, predominantly ranging from 2 to 50 nm, and (ii) macropores, spanning from 50 to 100 nm.

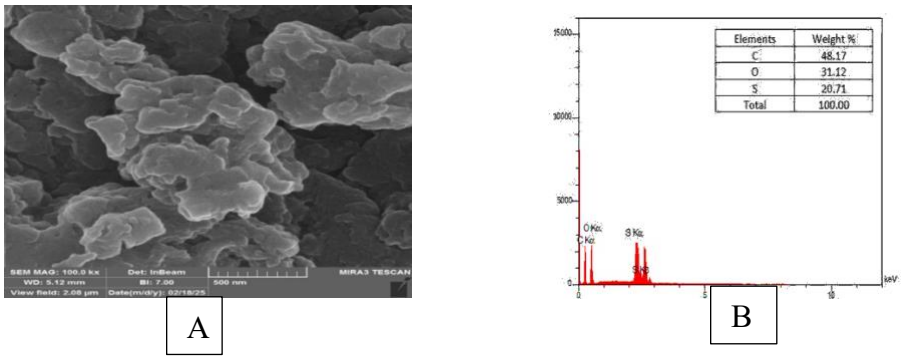

FIGURE 4 **(A)** SEM image illustrating the surface morphology of PEDOT, while **(B)** the elemental EDX spectrum of PEDOT.

The surface morphology of the produced PEDOT was investigated using field emission scanning electron microscopy (FE-SEM), as shown in **Fig. 4A**. The SEM of PEDOT displays a homogeneous, dense structure lacking a defined shape, characterized by aggregates with comparatively low porosity. The dimensions of the forms range from nanostructures to microstructures. Elemental analysis can determine the number of atoms in a sample and yield important information about the structure and composition of an adsorbent [35, 56]. **Fig. 4B** depicts the Energy Dispersive X-ray (EDX) analysis of the synthesized sample. The graphic demonstrates the presence of carbon, oxygen, and sulfur in the composition of PEDOT, indicating successful synthesis of the material. This result corroborates the successful synthesis of PEDOT and aligns with the FTIR and SEM data.

3.2 ADSORPTION STUDIES

3.2.1 IMPACT OF INITIAL SOLUTION PH

The protonation and/or deprotonation of the surface charge of adsorbent, in addition to the speciation of the pharmaceutical contaminants, depend on the pH of the solution. pH also impacts the adsorbent's ability by affecting the activity of its functional groups. The effect of pH on the removal of MET was investigated in this section using PEDOT adsorbent throughout a pH range of 2 to 10. The adsorbent dosage was 50 mg/L, the initial concentration for MET was 40 mg/L, and the duration was 120 minutes. The experimental results are illustrated in **Fig. 5**. This study revealed that the pH of the solution substantially affects the adsorption of MET. As pH rises, the adsorption efficacy for MET improves, as illustrated in **Fig. 5A**, with maximum removal efficiencies of 57.57% for MET at pH 6.

Determining the adsorbent's point of zero charge (pH_{pzc}) enables researchers to examine the charge behavior on the material's surface. This enables the identification of the pH at which the equilibrium of negative and positive charges is neutral. In other words, pH_{pzc} is an essential measure for comprehending the variations in surface charge with pH and its impact on the material's adsorption capacity, selectivity, and efficiency [59].

Fig. 5B indicates that the adsorbent's pH_{pzc} was 6.2. Below pH_{pzc}, the adsorbent surface exhibits a positive charge, while above the pH_{pzc}, it displays a negative charge. The pKa of metronidazole is 2.55 [14]. Consequently, this antibiotic possesses a positive charge in acidic pH due to its protonated form (MET-H^+). The adsorbent surface possesses a positive charge, resulting in repulsion between the two surfaces and diminishing adsorption between PEDOT and MET. At pH 6, attractive forces between PEDOT and the antibiotic MET are enhanced. In addition, other mechanisms for the adsorption of MET can be ascribed to π-π interactions and hydrogen bonding. As a result, pollutant adsorption within the adsorbent increases, enhancing removal efficiency. At pH values over pH_{pzc}, the adsorbent surface displays a negative charge in alkaline circumstances. Under this circumstance, metronidazole manifests as MET-OH^-, leading to repulsion between the adsorbent and the pollutant, hence diminishing the percentage removal. Subsequent research indicates that the ideal pH for the metronidazole adsorption process is within the neutral range [60, 61]. Furthermore, the lower percentage removal may also be due to H^+ ions competing for adsorption sites in an acidic environment (protonated drug) and OH^- ions competing in a basic environment (deprotonated drug). As a result, 6 was found to be the best pH for MET to adsorb onto PEDOT adsorbent.

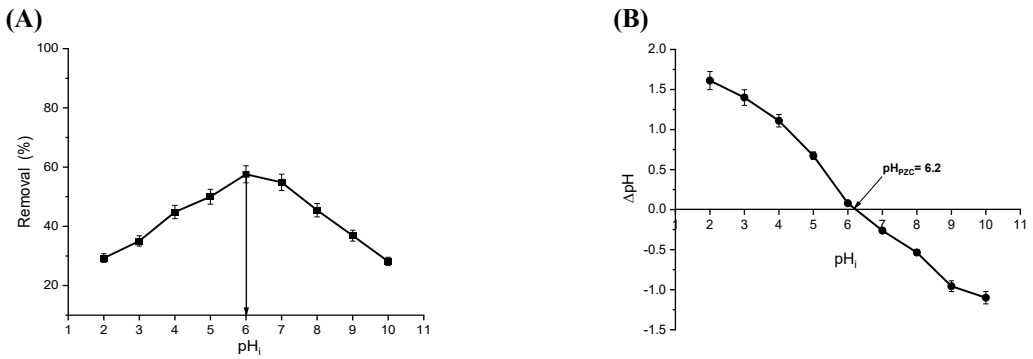

FIGURE 5 **(A)** The percentage of MET removed from solutions at various starting pHs (2–10) while maintaining all other parameters (conditions: beginning C_{drug} = 40 mg/L; V= 100 mL; temperature = 298 K, time = 120 min, dosage = 50 mg). **(B)** the pH_{pzc} analysis of the PEDOT adsorbent.

3.2.2 IMPACT OF ADSORBENT DOSAGE

The dosage of the adsorbent is a crucial practical aspect that significantly influences the removal rate and, consequently, the cost-effectiveness of the batch process. A dosage range of 10–140 mg was used to illustrate the impact of the adsorbent dose, while maintaining the same parameters (pH = 6, beginning drug concentration = 40 mg/L, volume = 100 mL, temperature = 298 K, treatment duration = 120 min). Using the PEDOT adsorbent, **Fig. 6A** shows how the adsorbent

dosage changes for the percentage removal of MET. These data show that when the amount of adsorbent was raised from 10 mg to 100 mg, the percentage removal for MET went from 14.5% to 61.2%; however, the percentage removal stayed constant beyond this point. A potential explanation for these results is that augmenting the dosage of the adsorbent will enhance the total number of accessible adsorption sites, hence enabling the adsorbent to eliminate a greater quantity of contaminants overall. As a result, the effectiveness of MET adsorption is improved. This results from the abundant presence of vacant adsorption sites, finally reaching a maximum at adsorption equilibrium.

3.2.3 IMPACT OF INITIAL CONCENTRATION

To optimize the interactions between pollutants in solution and adsorbent, modifications in initial concentration are essential for equilibrium studies. Under optimal testing circumstances (starting pH = 6, adsorbent dosage = 100 mg, duration = 120 min, and temperature = 298 K), the removal efficiency for MET adsorbed by the PEDOT adsorbent was assessed using varying initial concentrations of MET, from 20 to 200 mg/L. **Fig. 6B** demonstrates that the removal percentage of MET was consistent, at 62.1% for MET, despite an elevation in initial solution concentration from 20 to 100 mg/L. This is due to the unsaturated active sites on the adsorbent. Consequently, the clearance percentage decreased steadily from 62.1% to 31.7% for MET when drug concentration escalated from 120 to 200 mg/L. This indicates that increasing the solution concentration improves the potential transfer of drug ions to the adsorbent surface due to the heightened availability of functional groups, up to a certain maximum, beyond which it decreases. This transpires due to heightened drug concentrations, which intensify competition among molecules for the finite active adsorption sites on the adsorbent.

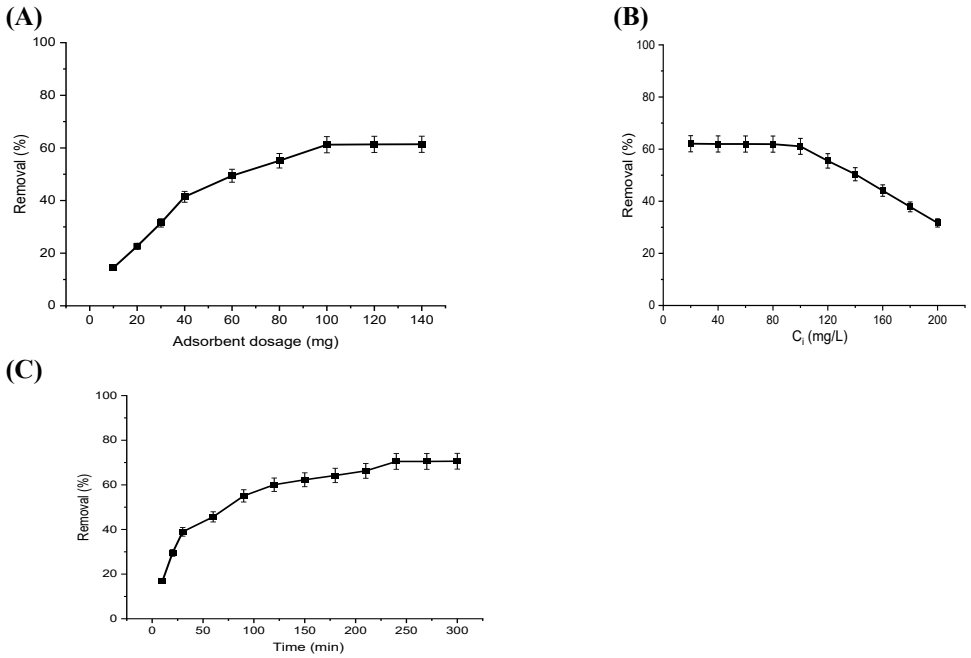

FIGURE 6 Impacts of **A)** adsorbent dosage (10 to 140 mg), **B)** initial MET concentration (20–200 mg/L), **C)** sorption time (10 – 300 min).

3.2.4 IMPACT OF REACTION TIME

Sorption time is considered to be one of the primary factors influencing drug adsorption. The pace at which equilibrium is reached and the equilibrium reaction time of the adsorption process are important variables in describing the adsorption mechanism in this case. The research examined the influence of adsorption period on the absorption of MET by the PEDOT adsorbent. Adsorption studies were conducted over a duration of 10 to 300 minutes, maintaining constant conditions (pH = 6, beginning drug concentration = 100 mg/L, volume = 100 mL, temperature = 298 K, adsorbent dosage = 100 mg), with results illustrated in **Fig. 6C**. The removal rate of MET utilizing PEDOT adsorbent rise with prolonged sorption period, ultimately attaining a peak level. As the adsorption time increases from 10 to 240 while using the PEDOT adsorbent, the removal rate of MET rise. The adsorption percentage of equilibrium after orbital shaking was 70.5% for MET. The rationale is that several sites on the adsorbent are available for adsorbate adsorption during the initial phases of the process. Further, this transpired due to drug molecules binding to functional groups, resulting in the near saturation of active adsorption sites on the PEDOT adsorbent. The velocity at which MET transitioned from the external to the inside pores of the nanocomposite's adsorbent particles dictated their adsorption rate. The sorption time for the succeeding trials was set at 240 minutes for MET due to the fact that the adsorption process reaches equilibrium.

3.3 ADSORPTION MODELLING STUDIES

3.3.1 KINETICS MODELLING STUDY

To assess the kinetic mechanism of MET's adsorption onto the PEDOT adsorbent, kinetic models such as pseudo-first-order, pseudo-secondary, and Elovich models were employed. The linear expression formulas for the different kinetic models are shown in **Table 1**. The pseudo-first-order model (**Eq. 4**) describes how the adsorbate only binds to one energetically homogenous, active location on the adsorbent surface, where interactions are physical in character. However, the pseudo-second-order model (**Eq. 5**) shows an analyte that can bind to two active groups with various binding energies and suggests that the adsorption process is chemical in nature [55]. **Eq. 6** specifies the Elovich model, which assumes a heterogeneous adsorbent surface, accounts for chemisorption-type adsorption, and suggests that adsorption occurs in multilayers [62, 63].

Table 1. Various kinetics model types.

Model	Linear Equation	Plot	Ref.
Pseudo-first-order	$ln(q_e - q_t) = lnq_e - k_1 t \ldots\ldots\ldots (4)$	$ln(q_e - q_t)\ vs. t$	[64]
pseudo-second-order	$\frac{t}{q_t} = \frac{1}{k_2 q_e^2} + \frac{t}{q_e} \ldots\ldots\ldots\ldots\ldots\ldots\ldots\ldots (5)$	$\frac{t}{q_t}\ vs.\ t$	[65]
Elovich	$q_t = \frac{1}{\beta} ln(\alpha\beta) + \frac{1}{\beta} ln\, t \ldots\ldots\ldots\ldots\ldots (6)$	$q_t\ vs. ln\, t$	[66]

Eq.4: q_e and q_t: the quantities of adsorbate adsorbed by the adsorbent (mg/g) at equilibrium and time t (min), respectively; k_1: the pseudo-first-order rate constant (min^{-1}). **Eq. 5:** k_2: the pseudo-second-order rate constant (mg/g min). **Eq. 6**: α: the initial adsorption rate constant (mg/g. min); β: desorption rate constant (g/mg).

As shown in **Fig. 7A-D**, the kinetic models were run with an initial drug concentration of 100 mg/L (with additional conditions mentioned in the caption). **Table 2** presents the theoretical and experimental outcomes obtained from the kinetic models. There are notable differences between qe generated from the pseudo-first-order models (**Fig. 7B**) and the experimentally determined equilibrium adsorption quantities (q_e exp.) of MET. The following are the MET values: q_e calculated = 70.5 mg/g and q_m experimental = 78.10 mg/g. Conversely, the pseudo-second-order model's (PSO) qe value for MET was 76.92 mg/g, closely aligning with the experimental findings. The experimental data (R^2) for MET align closely with the PSO model, yielding a coefficient of determination of 0.9977 for MET (**Fig. 7C**). This model, given by **Eq. 5**, considers that adsorption involves heterogeneous sites with differing energies and presumes chemical adsorption. The Elovich model asserts that the adsorbent's surface exhibits heterogeneous energy levels and involves a chemical adsorption mechanism. **Eq. 6** delineates the adsorption kinetics of this model. Incorporating the Elovich model into the pseudo-second-order model enhances its use by illustrating that the adsorption process may transpire in two distinct phases, each of which may be represented by two linear equations (see to **Fig. 7D**). The initial linear phase occurs when the analyte adheres to the exterior of the adsorbent, primarily on the PEDOT surface; the subsequent phase is characterized by a prolonged adsorption process, wherein the analyte attaches to particular spots or pores within the adsorbent [67]. The most representative adsorption process phase is the one that most closely matches the experimental data. The adsorption of MET by PEDOT demonstrated well-fitting linear segments, with R^2 values surpassing 0.9. The kinetic results demonstrate that the pseudo-second-order kinetic model produced superior correlation coefficient values ($R^2 > 0.99$). Moreover, the adsorption capacities calculated using the pseudo-second-order model (refer to **Table 2**) demonstrate a greater concordance with the experimental adsorption capabilities than those derived using the pseudo-first-order and Elovich models. Consequently, it can be inferred that MET is capable of adsorbing both internally and externally onto the material.

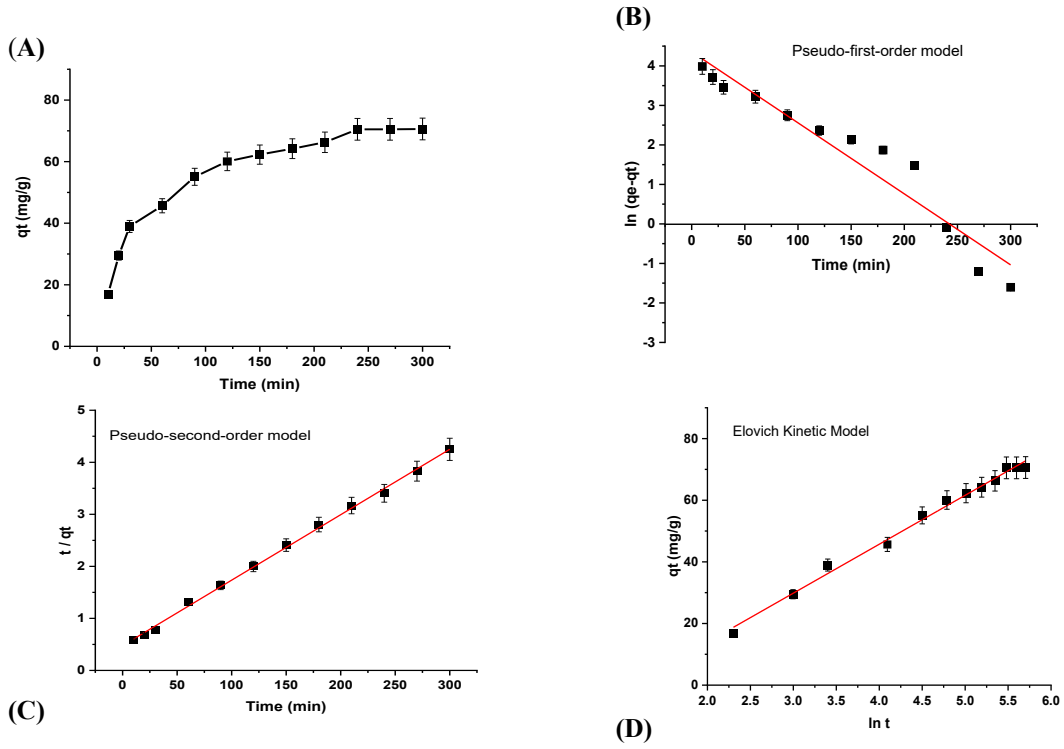

FIGURE 7 **A)** Effect of adsorption time: PEDOT adsorbent adsorption kinetics plots for adsorption of MET from solution at different sorption times; **B)** pseudo-first-order model; **C)** pseudo-second-order model; and **D)** Elovich model. Condition: (pH = 6, initial drug concentration = 100 mg/L, volume = 100 mL, temperature = 298 K, adsorbent dosage = 100 mg)

Table 2. Kinetics parameters of pseudo-first-order, pseudo-second-order, and Elovich, for MET adsorption by the PEDOT adsorbent (conditions: initial pH = 6; V = 100 mL; initial Ci = 100 mg/L; dose = 100 mg; T = 298 K).

Kinetic models	Parameter	Pharmaceutical MET
Pseudo-first-order	q_m *(exp.) (mg/g)*	70.50
	k_1 *(1/min)*	-0.00005
	q_e *cal.(mg/g)*	78.10
	R^2	0.9229
Pseudo-second-order	k_2 (mg/g.min)	0.00012
	q_e *cal.(mg/g)*	76.92
	R^2	0.9977
Elovich	α (mg/g.min)	0.3062
	β (g/mg)	0.0629
	R^2	0.9922

3.3.2 ISOTHERMAL MODELLING STUDY

Three significant theoretical models—the Langmuir [68], Freundlich [69], and the Temkin [70]— were employed to analyze the experimental results regarding the adsorption of MET, as well as the homogeneous and heterogeneous properties of the adsorbent. Isotherm adsorption tests were performed at initial MET concentrations between 20 and 200 mg/L at 298 K (**Fig. 8 A-D**, see to caption for further experimental conditions).

Table 3. Various isotherm model types.

Model	Linear Equation	Plot	References
Langmuir	$\frac{C_e}{q_e} = \frac{C_e}{q_m} + \frac{1}{q_m K_L}$ ... ...(7)	$\frac{C_e}{q_e}\ vs.\ C_e$	[68]
Freundlich	$lnq_e = lnK_F + \frac{1}{n} lnC_e$ ... ...(8)	$lnq_e\ vs.\ lnC_e$	[69]
Temkin	$q_e = A + B\ lnC_e$ ... ...(9)	$q_e\ vs.\ lnC_e$	[70]

Eq.7: q_e: the quantity of pharmaceutical adsorbed using the adsorbent at equilibrium (mg/g); C_e: the concentration of adsorbate at equilibrium (mg/L); q_{max}: the maximum adsorption capacity, as calculated from the Langmuir isotherm model (mg/g); K_L: Langmuir constant (L/mg). **Eq.8:** K_F: Freundlich constant (mg/g (L/mg)$^{1/n}$); n: heterogeneity constant.
Eq.9: B: the heat of sorption constant (J/mol); A: Temkin constant (L/g).

The Langmuir theoretical isotherm model has been used to describe adsorption processes that are both chemical and physical. It assumes that the drug molecules form a monolayer on the adsorption sites and that the outer surface of the adsorbent is uniform and regular [71]. Table 3 gives the linear mathematical expression (Eq. 7) for the Langmuir model. Graphing C_e/q_e vs C_e reveals a linear correlation, as illustrated in Fig. 8B. To determine the values of q_m and k_L, the graph's gradient and intercepts were utilized. The identified parameters are presented in Table 4 for MET drug. The appropriateness of the adsorption process was estimated isothermally using the Langmuir separation factor, R_L (R_L = 1/1+$K_L C_i$), whose value might be either irreversible (R_L = 0), unfavorable (R_L > 1), linear (R_L = 1), or favorable (0 < R_L < 1) [72]. According to the study, the MET R_L value fell between 0.0757 and 0.4505. This indicates that the PEDOT adsorbent is an advantageous method for attaching the MET drug.The Freundlich model can be characterized by a multilayer process, indicative of heterogeneous surfaces. This model is deficient as it fails to forecast the saturation of adsorption sites and may not adequately represent the process. Eq. 8 in Table 3 articulates the model linearly. Fig. 8C shows a plot of $ln\ q_e$ against $ln\ C_e$, which can be used to compute both K_f and n. The constant n is often utilized to denote the appropriateness of the adsorption process. The computed values of n, which fall between 1 and 10, is 2.1330 for MET (Table 4). This value shows that the drug adsorption onto the PEDOT adsorbent is favorable. The Temkin isotherm model controls a linear decrease in the adsorption energy with an increase in the surface area of the adsorbent. It also considers the interaction between the adsorbent and the adsorbate. Table 3 delineates the linear mathematical formulation of the Temkin model (Eq. 9). The constants A and B can be derived from a plot of q_e versus $ln\ C_e$ (Fig. 8 D). The isotherm factors for the adsorption of MET are presented in Table 4.

Table 4 shows the model that produced the best match by displaying the model factors computed for each theoretical isotherm model together with the corresponding R^2 values. According to the study, the experimental adsorption capacity was (q_m (exp.) = 86.80 mg/g) and the Langmuir model's adsorption capacity was (q_m (cal.) = 77.66 mg/g). This contrasted with the results of the Freundlich and Temkin models. Furthermore, the R^2 values presented in **Table 4** indicate that the theoretical Langmuir model offers the most accurate fit to the data (R^2 > 0.97). Nevertheless, the Temkin and Freundlich models indicated that the R^2 values for MET pharmaceutical inadequately aligned with the experimental results. Consequently, it was concluded that, unlike the Freundlich or Temkin models, the theoretical Langmuir model most accurately characterizes the MET adsorption process. The adsorption mechanism of MET on the PEDOT adsorbent follows a monolayer adsorption model.

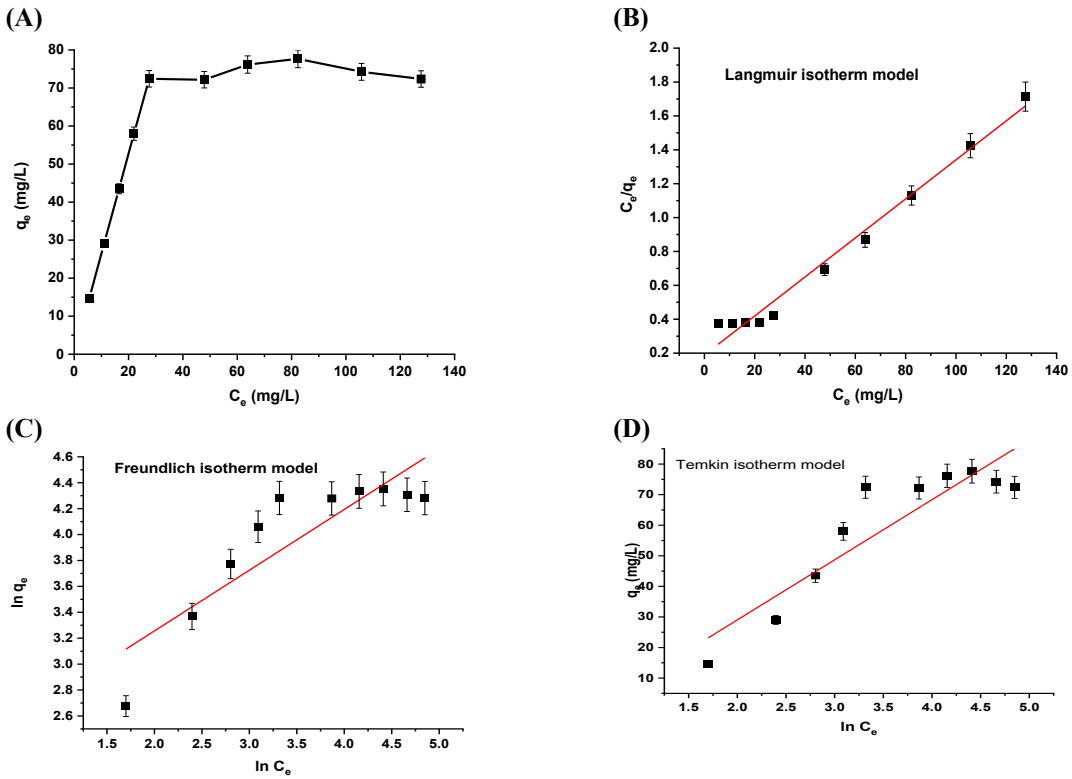

FIGURE 8 (**A**) Adsorption isotherm studies for the adsorption of MET by the PEDOT adsorbent (conditions: initial pH = 6; dose = 100 mg; time = 240 min for MET; V = 100 mL; T = 298 K), fitted to (**B**) Langmuir, (**C**) Freundlich, and (**D**) Temkin models.

Table 4. Adsorption isotherm parameters for the Langmuir, Freundlich, and Temkin models for the adsorption of MET by the PEDOT adsorbent (conditions: initial pH = 6 for MET; V = 100 mL; dose = 100 mg; time = 240 min; T = 298 K).

Isotherm models	Parameter	Pharmaceutical MET
	q_m (exp.) (mg/g)	77.66
Langmuir	q_m (mg/g)	86.80
	K_L(L/mg)	0.061
	R_L range	0.0757– 0.4505
	R^2	0.9797
Freundlich	K_F (mg/g (L/mg)$^{1/n}$)	208.27
	n	2.1330
	R^2	0.7713
Temkin	A	0.592
	B	19.65
	R^2	0.8072

3.4 COMPARISON OF VARIOUS ADSORBENTS

Table 5 lists the adsorption capacity (q_m) of PEDOT and other optimal adsorption settings, which are used to evaluate its capability to remove MET to that of other known adsorbents. The high q_m (86 mg/g) of the PEDOT adsorbent for MET adsorption makes it a potential choice for wastewater treatment. The PEDOT's in-situ polymerization produces unique morphologies with a very high specific surface area and mesoporous properties that are necessary for improved drug adsorption. Moreover, interactions between MET molecules and the adsorbent surface through hydrogen bonding and π-π interactions are anticipated during the adsorption process of MET.

Table 5. Comparison of various adsorbents used for adsorption MET contaminant from wastewater.

Adsorbents	Pharma-ceuticals	Parameters				Kinetic model	Isotherm model	Adsorption capacities (mg/g)	Ref.
		pH	Time (h)	Dose (g/L)	Conc. (mg/L)				
Polypyrrole	MET	6.2	2.0	0.5	1	PSO	Langmuir	5.05	[48]
$CoFe_2O_4$/activated-carbon@ chitosan as magnetic biocomposite	MET	5.0	0.77	0.45	22.35		Freundlich	36.897	[73]
PPy-PANI copolymer	MET	6.2	5.0	0.4	10	PFO	Freundlich	63.84	[14]
$FeNi_3/SiO_2$/CuS magnetic nanocomposite	MET	7.0	3.0	0.1	20	PSO	Langmuir	135	[13]
MgO/LECA nanocomposite	MET	7.0	-	1	40	PSO	Langmuir	84.55	[74]
PEDOT	MET	6	4	0.1	100	PSO	Langmuir	86.80	This work

* PNO = pseudo-nth order model, PFO = pseudo-first-order, PSO = pseudo-second-order

3.5 Impact of reaction temperature and thermodynamic studies

The temperature of the reaction is another significant aspect that can modify the removal method. According to ideal circumstances from earlier experiments, the reaction temperature was maintained with an adsorbent dosage of 100 mg in drug solution (100 mg/L) at an initial pH of 6 and reaction durations of 240 minutes. **Fig. 9A** demonstrates the influence of temperature on the capacity of PEDOT to eliminate MET; additionally, it is evident that the removal percentage (R%) increased from 70.5% to 80.2% for MET as the temperature ascended from 298 to 313 K. The information indicates that the pharmacological reaction in this study is endothermic [75]. According to this finding, the percentage elimination increases with the reaction temperature, peaking at 313 K. The reason for this is because the drug ions are more mobile and would have enough energy to interact with the accessible sites on the surface of the nanocomposite. The Van't Hoff equation (**Eq. 10**) can be used to find the standard Gibbs free energy ($\Delta G°$(J/mol)), the standard entropy change ($\Delta S°$ (J/mol)), and the standard enthalpy change ($\Delta H°$ (J/mol K)) [76], for the MET adsorption processes via PEDOT.

$$ln(K_L) = -\frac{\Delta H^{\circ}}{RT} + \frac{\Delta S^{\circ}}{R} \quad (10)$$

Here, R represents the universal gas constant (8.314 J/mol K), while K_L indicates the Langmuir equilibrium constant (L/mg), and T is the absolute temperature (K). $\Delta H°$ and $\Delta S°$ were obtained from **Fig. 9B**, from the slope and intercept of the linear equation of ln K_L versus 1/T. $\Delta G°$ was calculated at each of the four designated temperatures (298, 303, 308, and 313 K) using **Eq. 11**.

$$\Delta G^{\circ} = -RTln(K_L) \quad (11)$$

The thermodynamic parameters ΔH^o, ΔS^o, and ΔG^o for MET adsorption onto the PEDOT adsorbent system have been calculated, as reported in **Table 8**. For the MET adsorption process, ΔH^o and ΔS^o are determined to be 29.00 kJ/mol and 11.97 J/mol K, respectively. Further, ΔG^o was obtained to be -2.158, -2.556, -3.331, and -3.640 kJ/mol, at temperatures of 298, 305, 303, and 313 K, respectively. The data presented in **Table 6** demonstrate that the negative ΔG^o ($\Delta G^o < 0$) and positive ΔH^o ($\Delta H^o > 0$) values signify that the adsorption of MET onto PEDOT is both endothermic and spontaneous. Additionally, during the adsorption of the MET solution, which was the adsorbate, the solid adsorbent (PEDOT) showed randomization at the solid–solution interface, as evidenced by the positive entropy value ($\Delta S > 0$). Similar results have been documented in previous studies [12, 13]. In addition, enthalpy (ΔH^o) provides information regarding the type of adsorption, including whether it is more likely to be chemical/physisorption (40–800 kJ/mol) or physical/physisorption (0–40 kJ/mol) [77, 78].The high ΔH^o (29.00 kJ/mol) obtained for MET pointed to physisorption.

3.6 REUSABILITY STUDIES OF PEDOT ADSORBENT

One important feature of the adsorbent is its reusability. The reusability of PEDOT was therefore examined in order to assess the adsorption efficiency after several cycles of use. **Fig. 10** demonstrates the reusability of PEDOT for the adsorption of MET throughout five cycles. The adsorbent was subjected to centrifugation and filtration following the initial cycle and subsequently washed with methanol. Subsequently, it was employed as the adsorbent for further cycles

to assess its adsorptive performance following a three-hour drying period at 80°C in a vacuum oven. Figure 10 illustrates

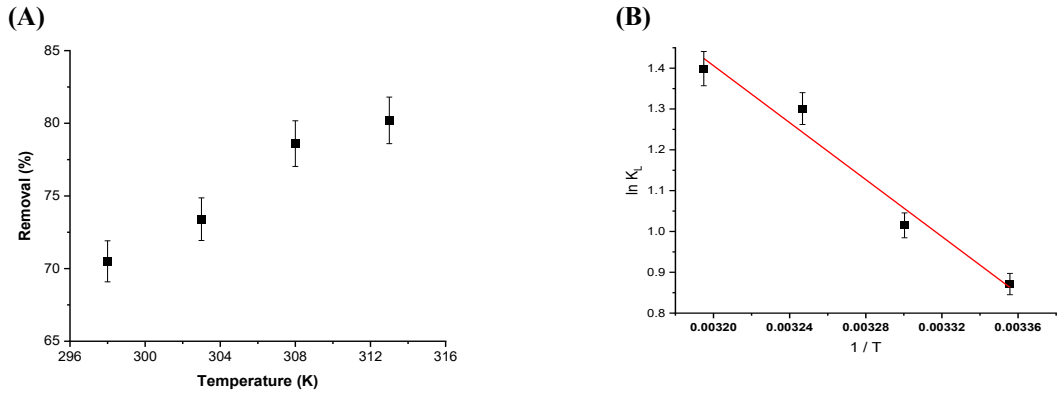

FIGURE 9. **(A)** Impact of reaction temperature on adsorption of MET onto the PEDOT adsorbent at four temperatures (298, 303, 308, and 313 K), **(B)** Linear plot of ln K_L against 1/T for adsorption of MET onto the adsorbent PEDOT adsorbent.

Table 8. Thermodynamic parameters found for adsorption of MET onto the PEDOT adsorbent at four temperatures (298, 303, 308, and 313 K). (Fixed conditions: pH = 6; V = 100 mL; dosages = 100 mg; time = 240 min).

Pharmaceutical	Thermodynamic Parameter	Temperatures of reaction (K)			
		298	303	308	313
MET	$\Delta G°$ (KJ/mol)	-2.158	-2.556	-3.331	-3.640
	$\Delta H°$ (KJ/mol)	29.00			
	$\Delta S°$ (J/mol)	11.97			

reduction in MET adsorption from 71.33% to 51.58% at an initial adsorbate concentration of 100 mg/L; similarly, the desorption test indicated a decline from 63.1% to 47.0%. A persistent decrease in the adsorbent's adsorption-desorption efficiency could indicate that there is still MET present on the adsorbent. Up to five successful recycling cycles are possible with PEDOT adsorbent.

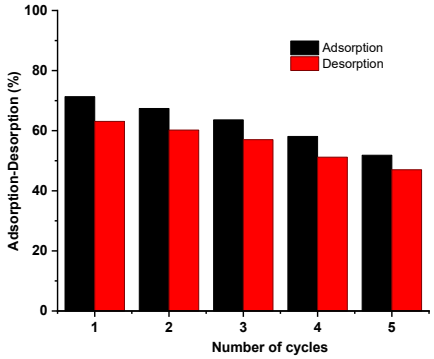

FIGURE 10. Adsorption–desorption cycles for MET loading onto PEDOT adsorbent.

CONCLUSION

This study describes the batch adsorption of metronidazole onto a PEDOT adsorbent derived from oxaline-DES. Several techniques, including FTIR, SEM, BET, and EDX were utilized to characterize the PEDOT adsorbent. The formation of PEDOT adsorbent was confirmed by FTIR, SEM, and EDX. The BET surface area measurement indicates that the PEDOT adsorbent consists of nanosized particles. The effects of initial pH, PEDOT dose, initial drug concentration, temperature, and contact time on MET adsorption were investigated. It was found that MET drug adsorption onto the PEDOT adsorbent increases with rising pH, reaching a maximum at pH 6. After this, adsorption efficiency starts to decline. It was found that the adsorption of MET had an equilibrium duration of 240 minutes.

The adsorption isotherms for the MET pharmaceutical on the adsorbent's surface indicated that the Langmuir isotherm was the most suitable model at 298 K. The highest adsorption capacity of MET was 86.80 mg/g. The R^2 value for MET about the Langmuir isotherm was 0.9797, indicating that adsorption occurred uniformly and in a monolayer on the adsorbent surface. A pseudo-second-order mechanism was determined to best suit the MET drug's adsorption kinetics ($R^2 = 0.9977$). Furthermore, as the amount of adsorption increased with temperature, thermodynamic data suggested that the adsorption process was endothermic. Furthermore, the free energy (ΔG) for the adsorption of the MET drug was negative, indicating a spontaneous response. In addition, the enthalpy of MET was 29.00 kJ/mol, signifying that the adsorption was of a physical character. The adsorption-desorption analysis indicated a decrease in the adsorption capacity for MET from 71.33% to 51.58% after five cycles. These findings underscore the efficacy of PEDOT as an absorbent for the efficient adsorption of MET from aqueous solutions.

FUNDING

This research is part of the requirements for a master's degree (H. H. Abdulrahman). Therefore, the authors declare that no funds, grants, or other support were received during the preparation of this manuscript

ACKNOWLEDGEMENT

The authors wish to acknowledge Koya and Kashan Universities for supplying the necessary supplies and instruments for this research.

CONFLICTS OF INTEREST

The authors declare no conflict of interest.

DATA AVAILABILITY

The corresponding author can provide the data and data sets created during the current investigation upon reasonable request.

REFERENCES

[1] H. de Oliveira Souza, R. dos Santos Costa, G. R. Quadra, and M. A. dos Santos Fernandez, "Pharmaceutical pollution and sustainable development goals: Going the right way?," Sustainable Chemistry and Pharmacy, vol. 21, p. 100428, 2021.

[2] M. Le Moal, C. Gascuel-Odoux, A. Ménesguen, Y. Souchon, C. Étrillard, A. Levain, et al., "Eutrophication: a new wine in an old bottle?," Science of the total environment, vol. 651, pp. 1-11, 2019.

[3] N. G. Kandile and A. S. Nasr, "New hydrogels based on modified chitosan as metal biosorbent agents," International journal of biological macromolecules, vol. 64, pp. 328-333, 2014.

[4] X. Zhang, C. M. Navarathna, W. Leng, T. Karunaratne, R. V. Thirumalai, Y. Kim, et al., "Lignin-based few-layered graphene-encapsulated iron nanoparticles for water remediation," Chemical Engineering Journal, vol. 417, p. 129199, 2021.

[5] A. F. H. Sdiq, H. H. Abdulrahman, H. K. Ismail, R. A. Omer, H. F. Alesary, H. K. I. Sultan, et al., "A Review of Effective Nanoadsorbents Made of Carbonaceous, Metal Oxides, and Polymer Nanocomposite Materials for Adsorption of Pharmaceutical Contaminants in Wastewater," International Journal of Environmental Research, vol. 19, p. 159, 2025.

[6] H. H. Abdulrahman, A. F. H. Sdiq, H. K. Ismail, R. A. Omer, H. F. Alesary, A. A. Kareem, et al., "Polymer Nanocomposite Adsorbents for the Removal of Pharmaceutical Formulations the Aquatic Environment: A Review," Water, Air, & Soil Pollution, vol. 236, p. 584, 2025.

[7] S. Klatte, H. C. Schaefer, and M. Hempel, "Pharmaceuticals in the environment–a short review on options to minimize the exposure of humans, animals and ecosystems," Sustainable Chemistry and Pharmacy, vol. 5, pp. 61-66, 2017.

[8] I. T. Carvalho and L. Santos, "Antibiotics in the aquatic environments: a review of the European scenario," Environment international, vol. 94, pp. 736-757, 2016.

[9] P. Grenni, V. Ancona, and A. B. Caracciolo, "Ecological effects of antibiotics on natural ecosystems: A review," Microchemical Journal, vol. 136, pp. 25-39, 2018.

[10] I. B. Qader, A. R. Ganjo, H. O. Ahmad, H. A. Qader, and H. A. Hamadameen, "Antibacterial and Antioxidant Study of New Pharmaceutical Formulation of Didecyldimethylammonium Bromide Via Pharmaceutical Deep Eutectic Solvents (PDESs) Principle," AAPS PharmSciTech, vol. 25, p. 25, 2024.

[11] D. T. Ruziwa, A. E. Oluwalana, M. Mupa, L. Meili, R. Selvasembian, M. M. Nindi, et al., "Pharmaceuticals in wastewater and their photocatalytic degradation using nano-enabled photocatalysts," Journal of Water Process Engineering, vol. 54, p. 103880, 2023.

[12] J. A. War and H.-T.-N. Chisti, "Synthesis, characterization, and application of a zinc oxide–pyrrole–thiophene nanocomposite as an efficient adsorbent for the removal of tetracycline," New Journal of Chemistry, vol. 47, pp. 16399-16414, 2023.

[13] N. Nasseh, B. Barikbin, L. Taghavi, and M. A. Nasseri, "Adsorption of metronidazole antibiotic using a new magnetic nanocomposite from simulated wastewater (isotherm, kinetic and thermodynamic studies)," Composites Part B: Engineering, vol. 159, pp. 146-156, 2019.

[14] N. Aarab, A. Hsini, A. Essekri, M. Laabd, R. Lakhmiri, and A. Albourine, "Removal of an emerging pharmaceutical pollutant (metronidazole) using PPY-PANi copolymer: kinetics, equilibrium and DFT identification of adsorption mechanism," Groundwater for Sustainable Development, vol. 11, p. 100416, 2020.

[15] H. K. Ismail, A. F. Qader, R. A. Omer, H. F. Alesary, H. M. Umran, and A. A. Kareem, "Synthesis of Polypyrrole-Graphene Oxide (PPy/GO) from Deep Eutectic Solvent and Its Characterization for Determination of Metronidazole Pharmaceutical Substance Using Spectrofluorometric Technique," ChemistrySelect, vol. 10, p. e202405486, 2025.

[16] N. Neghi, N. R. Krishnan, and M. Kumar, "Analysis of metronidazole removal and micro-toxicity in photolytic systems: Effects of persulfate dosage, anions and reactor operation-mode," Journal of environmental chemical engineering, vol. 6, pp. 754-761, 2018.

[17] F. Desbiolles, L. Malleret, C. Tiliacos, P. Wong-Wah-Chung, and I. Laffont-Schwob, "Occurrence and ecotoxicological assessment of pharmaceuticals: is there a risk for the Mediterranean aquatic environment?," Science of the Total Environment, vol. 639, pp. 1334-1348, 2018.

[18] S. M. Bekhit, S. A. Zaki, M. S. E.-D. Hassouna, and M. Elkady, "Effectiveness of fullerene/magnesium oxide nanocomposite in removing ciprofloxacin and tetracycline from aqueous solutions," RSC advances, vol. 15, pp. 5190-5201, 2025.

[19] A. K. Mohammed, S. M. Saadoon, Z. T. Abd Ali, I. M. Rashid, and N. H. A. Sbani, "Removal of amoxicillin from contaminated water using modified bentonite as a reactive material," Heliyon, vol. 10, 2024.

[20] R. Kasraei and M. Malakootian, "Tetracycline adsorption from aqueous solutions by a magnetic nanoadsorbent modified with ionic liquid," Desalination and Water Treatment, vol. 209, pp. 289-301, 2021.

[21] M. K. Mohammadi Nodeh, S. Soltani, S. Shahabuddin, H. Rashidi Nodeh, and H. Sereshti, "Equilibrium, kinetic and thermodynamic study of magnetic polyaniline/graphene oxide based nanocomposites for ciprofloxacin removal from water," Journal of Inorganic and Organometallic Polymers and Materials, vol. 28, pp. 1226-1234, 2018.

[22] A. M. Aljeboree and A. N. Alshirifi, "Adsorption of Pharmaceuticals as emerging contaminants from aqueous solutions on to friendly surfaces such as activated carbon: A review," Journal of Pharmaceutical Sciences and Research, vol. 10, pp. 2252-2257, 2018.

[23] H. Abd-ElFattah, R. M. Kamel, and A. Maged, "Harnessing clays and clay composites for efficient removal of pharmaceutical contaminants from water: A review," Frontiers in Scientific Research and Technology, 2025.

[24] S. Álvarez, R. S. Ribeiro, H. T. Gomes, J. L. Sotelo, and J. García, "Synthesis of carbon xerogels and their application in adsorption studies of caffeine and diclofenac as emerging contaminants," Chemical Engineering Research and Design, vol. 95, pp. 229-238, 2015.

[25] S. Amirshekari, S. Shafiei, M. Zahedifar, and H. Shekofteh, "Development of functionalized biochar composites for enhanced boron adsorption from aqueous solutions," Heliyon, vol. 11, 2025.

[26] J. Aslam, S. Zehra, M. Mobin, M. Quraishi, C. Verma, and R. Aslam, "Metal/metal oxide-carbohydrate polymers framework for industrial and biological applications: Current advancements and future directions," Carbohydrate Polymers, vol. 314, p. 120936, 2023.

[27] M. Papageorgiou, K. N. Maroulas, E. Evgenidou, D. N. Bikiaris, G. Z. Kyzas, and D. A. Lambropoulou, "Simultaneous Removal of Seven Pharmaceutical Compounds from a Water Mixture Using Modified Chitosan Adsorbent Materials," Macromol, vol. 4, pp. 304-319, 2024.

[28] A. A. Attia, T. E. Khalil, H. A. Elbadawy, A. Tawfik, D. S. El-Sayed, and A. El-Dissouky, "Effective removal of tetracycline from wastewater using carbonaceous materials derived from Brassica oleracea plant: Experimental and computational perturbation," Journal of Molecular Liquids, p. 127106, 2025.

[29] G. M. M. Demiti, Y. J. Fachina, E. F. D. Januário, M. H. N. O. Scaliante, M. T. Rodríguez, and R. Bergamasco, "Removing pharmaceuticals from water with natural and modified zeolites: Kinetics, thermodynamics, and competitive adsorption in a multi-drug system," Journal of Molecular Liquids, vol. 418, p. 126688, 2025.

[30] H. L. de Oliveira, B. C. Pires, L. S. Teixeira, L. A. F. Dinali, T. A. do Nascimento, and K. B. Borges, "Mesoporous molecularly imprinted polymer for removal of hormones from aqueous medium," Colloids and Surfaces A: Physicochemical and Engineering Aspects, vol. 590, p. 124506, 2020.

[31] S. Dutta, S. K. Srivastava, B. Gupta, and A. K. Gupta, "Hollow Polyaniline Microsphere/MnO2/Fe3O4 Nanocomposites in Adsorptive Removal of Toxic Dyes from Contaminated Water," ACS Applied Materials & Interfaces, vol. 13, pp. 54324-54338, 2021.

[32] H. M. Umran, H. F. Alesary, H. K. Ismail, F. Wang, and S. Barton, "Influence of surface chemical modifications on enhancing the aging behavior of capacitor biaxially-oriented polypropylene thin film," Polymer Degradation and Stability, vol. 231, p. 111105, 2025.

[33] M. B. Hasan, M. M. Parvez, A. Y. Abir, and M. F. Ahmad, "A Review on Conducting Organic Polymers: Concepts, Applications, and Potential Environmental Benefits," Heliyon, 2025.

[34] I. B. Qader, H. K. Ismail, H. F. Alesary, J. H. Kareem, Y. T. Maaroof, and S. Barton, "Electrochemical sensor based on polypyrrole/triiron tetraoxide (PPY/Fe3O4) nanocomposite deposited from a deep eutectic solvent for voltammetric determination of procaine hydrochloride in pharmaceutical formulations," Journal of Electroanalytical Chemistry, vol. 951, p. 117943, 2023.

[35] J. M. Alshawi, M. Q. Mohammed, H. F. Alesary, H. K. Ismail, and S. Barton, "Voltammetric Determination of Hg2+, Zn2+, and Pb2+ Ions Using a PEDOT/NTA-Modified Electrode," ACS Omega, vol. 7, pp. 20405–20419, 2022.

[36] M. Q. Mohammed, H. K. Ismail, H. F. Alesary, and S. Barton, "Use of a Schiff base-modified conducting polymer electrode for electrochemical assay of Cd (II) and Pb (II) ions by square wave voltammetry," Chemical Papers, vol. 76, pp. 715-729, 2022.

[37] H. K. Ismail, H. F. Alesary, J. A. Juma, A. R. Hillman, and K. S. Ryder, "A comparative study of the formation, and ion and solvent transport of polyaniline in protic liquid-based deep eutectic solvents and aqueous solutions using EQCM," Electrochimica Acta, vol. 418, p. 140348, 2022.

[38] H. Ismail, R. Omer, Y. Azeez, K. Omar, and H. Alesary, "Synthesis, Characterization, and Computational Insights Into the Conductive Poly (p-aminophenol)," Russian Journal of Physical Chemistry B, vol. 18, pp. 1148-1165, 2024.

[39] V. Gayathri and R. Balan, "Synthesis and Characterisation of Inorganic Acid Doped Conducting Polymer," J. Environ. Nanotechnol, vol. 8, pp. 20-23, 2019.

[40] H. F. Alesary, H. K. Ismail, M. Q. Mohammed, H. N. Mohammed, Z. K. Abbas, and S. Barton, "A comparative study of the effect of organic dopant ions on the electrochemical and chemical synthesis of the conducting polymers polyaniline, poly (o-toluidine) and poly (o-methoxyaniline)," Chemical Papers, vol. 75, pp. 5087-5101, 2021.

[41] Y. T. Maaroof, I. B. Qader, H. K. Ismail, H. Q. Hamad, and S. R. Taher, "Extraction of Sulfur Compounds from Model Petroleum Products using Fe3O4 Nanoparticles and Acetic Acid-1-Butyl-3-Methylimidazolium Chloride based on Deep Eutectic Solvents," ARO-THE SCIENTIFIC JOURNAL OF KOYA UNIVERSITY, vol. 12, pp. 254-263, 2024.

[42] A. P. Abbott, G. Capper, D. L. Davies, R. K. Rasheed, and V. Tambyrajah, "Novel solvent properties of choline chloride/urea mixtures," Chemical Communications, pp. 70-71, 2003.

[43] I. B. Qader, "Enhance dissolution rate and solubility of solid drugs through pharmaceutical deep eutectic solvents," Zanco Journal of Pure and Applied Sciences, vol. 33, pp. 98-106, 2021.

[44] H. F. Alesary, H. K. Ismail, J. H. Kareem, I. B. Qader, A. H. Odda, A. F. Halbus, et al., "Characterization of the electrochemical deposition of aluminum from an AlCl3: N-methylacetamide eutectic solvent modified with nicotinamide," Surface and Coatings Technology, vol. 475, p. 130160, 2023.

[45] N. A. Husin, M. Muhamad, N. Yahaya, M. Miskam, N. N. S. N. M. Kamal, S. Asman, et al., "Application of a new choline-imidazole based deep eutectic solvents in hybrid magnetic molecularly imprinted polymer for efficient and selective removal of naproxen from aqueous samples," Materials Chemistry and Physics, vol. 261, p. 124228, 2021.

[46] A. Bano, B. Prasad, H. Dave, and K. S. Prasad, "A mechanistic insight on non-steroidal anti-inflammatory drug, ketoprofen removal from pharmaceutical wastewater by a magnetic biochar: Batch and fixed bed adsorption studies," Inorganic Chemistry Communications, vol. 173, p. 113802, 2025.

[47] E. Asgari, A. Sheikhmohammadi, and J. Yeganeh, "Application of the Fe3O4-chitosan nano-adsorbent for the adsorption of metronidazole from wastewater: Optimization, kinetic, thermodynamic and equilibrium studies," International Journal of Biological Macromolecules, vol. 164, pp. 694-706, 2020.

[48] N. Aarab, M. Laabd, H. Eljazouli, R. Lakhmiri, H. Kabli, and A. Albourine, "Experimental and DFT studies of the removal of pharmaceutical metronidazole from water using polypyrrole," International Journal of Industrial Chemistry, vol. 10, pp. 269-279, 2019.

[49] C. O. Aniagor and M. C. Menkiti, "Analysis of metronidazole adsorption onto cellulose-chitosan composite adsorbent," UNIZIK Journal of Engineering and Applied Sciences, vol. 3, pp. 1307-1316, 2024.

[50] C. Zheng, M. Du, F. Li, Y. Qi, and J. Yi, "Selective adsorption of metronidazole on conjugated microporous polymers," Science China Chemistry, vol. 58, pp. 1227-1234, 2015.

[51] S. S. Alabdullah, H. K. Ismail, K. S. Ryder, and A. P. Abbott, "Evidence supporting an emulsion polymerisation mechanism for the formation of polyaniline," Electrochimica Acta, vol. 354, p. 136737, 2020.

[52] A. R. Hillman, K. S. Ryder, H. K. Ismail, A. Unal, and A. Voorhaar, "Fundamental aspects of electrochemically controlled wetting of nanoscale composite materials," Faraday discussions, vol. 199, pp. 75-99, 2017.

[53] R. A. Omer, H. K. Ismail, H. K. Sultan, H. F. Alesary, A. A. Kareem, Y. H. Azeeza, et al., "Synthesis of polyaniline, polypyrrole, and poly (aniline-co-pyrrole) in deep eutectic solvent: a comparative experimental and computational investigation of their structural, spectral, thermal, and morphological characteristics," Chemistry of Heterocyclic Compounds, vol. 60, pp. 463–472, 2024.

[54] H. K. Ismail, H. F. Alesary, and M. Q. Mohammed, "Synthesis and characterisation of polyaniline and/or MoO2/graphite composites from deep eutectic solvents via chemical polymerisation," Journal of Polymer Research, vol. 26, p. 65, 2019.

[55] T. A. Nascimento, B. C. Pires, F. V. A. Dutra, M. M. C. Borges, and K. B. Borges, "Poly (aniline-co-pyrrole) as Adsorbent for Removal of Pharmaceuticals: Preparation, Characterization, Kinetics, Isotherms and Application on Sample Preparation," ChemistrySelect, vol. 9, p. e202305101, 2024.

[56] S. Ghosh, A. K. Mallik, and R. N. Basu, "Enhanced photocatalytic activity and photoresponse of poly(3,4-ethylenedioxythiophene) nanofibers decorated with gold nanoparticle under visible light," Solar Energy, vol. 159, pp. 548-560, 2018.

[57] R. Kumar, A. Akbarinejad, T. Jasemizad, R. Fucina, J. Travas-Sejdic, and L. P. Padhye, "The removal of metformin and other selected PPCPs from water by poly(3,4-ethylenedioxythiophene) photocatalyst," Science of The Total Environment, vol. 751, p. 142302, 2021.

[58] K. N. Kim, H.-R. Jung, and W.-J. Lee, "Hollow cobalt ferrite–polyaniline nanofibers as magnetically separable visible-light photocatalyst for photodegradation of methyl orange," Journal of Photochemistry and Photobiology A: Chemistry, vol. 321, pp. 257-265, 2016.

[59] B. Carneiro Pires, F. V. Avelar Dutra, T. Aparecida Nascimento, and K. Bastos Borges, "Removal of pharmaceuticals from aqueous samples by adsorption using pristine polypyrrole as adsorbent: kinetic, isothermal and thermodynamic studies," International Journal of Environmental Analytical Chemistry, vol. 103, pp. 5337-5354, 2023.

[60] M. Farzadkia, A. Esrafili, M. A. Baghapour, Y. D. Shahamat, and N. Okhovat, "Degradation of metronidazole in aqueous solution by nano-ZnO/UV photocatalytic process," Desalination and Water Treatment, vol. 52, pp. 4947-4952, 2014.

[61] D. H. Carrales-Alvarado, R. Ocampo-Pérez, R. Leyva-Ramos, and J. Rivera-Utrilla, "Removal of the antibiotic metronidazole by adsorption on various carbon materials from aqueous phase," Journal of Colloid and Interface Science, vol. 436, pp. 276-285, 2014.

[62] H. K. Ismail, L. I. A. Ali, H. F. Alesary, B. K. Nile, and S. Barton, "Synthesis of a poly (p-aminophenol)/starch/graphene oxide ternary nanocomposite for removal of methylene blue dye from aqueous solution," Journal of Polymer Research, vol. 29, pp. 1-22, 2022.

[63] L. A. Ali, H. K. Ismail, H. F. Alesary, and H. Aboul-Enein, "A nanocomposite based on polyaniline, nickel and manganese oxides for dye removal from aqueous solutions," International Journal of Environmental Science and Technology, vol. 18, pp. 2031-2050, 2021.

[64] S. K. Lagergren, "About the theory of so-called adsorption of soluble substances," Sven. Vetenskapsakad. Handingarl, vol. 24, pp. 1-39, 1898.

[65] G. McKay, Y. Ho, and J. Ng, "Biosorption of copper from waste waters: a review," Separation and Purification Methods, vol. 28, pp. 87-125, 1999.

[66] S. Y. Elovich and G. Zhabrova, "Mechanism of the catalytic hydrogenation of ethylene on nickel. I. Kinetics of the process," Journal of Physical Chemistry, vol. 13, p. 1761, 1939.

[67] W. Rudzinski and W. Plazinski, "Theoretical description of the kinetics of solute adsorption at heterogeneous solid/solution interfaces: On the possibility of distinguishing between the diffusional and the surface reaction kinetics models," Applied Surface Science, vol. 253, pp. 5827-5840, 2007.

[68] I. Langmuir, "The constitution and fundamental properties of solids and liquids. Part I. Solids," Journal of the American chemical society, vol. 38, pp. 2221-2295, 1916.

[69] H. Freundlich, "Über die adsorption in lösungen," Zeitschrift für physikalische Chemie, vol. 57, pp. 385-470, 1907.

[70] M. Tempkin and V. Pyzhev, "Kinetics of ammonia synthesis on promoted iron catalyst," Acta Phys. Chim. USSR, vol. 12, p. 327, 1940.

[71] K. L. Yu, X. J. Lee, H. C. Ong, W.-H. Chen, J.-S. Chang, C.-S. Lin, et al., "Adsorptive removal of cationic methylene blue and anionic Congo red dyes using wet-torrefied microalgal biochar: Equilibrium, kinetic and mechanism modeling," Environmental pollution, vol. 272, p. 115986, 2021.

[72] R. Foroutan, R. Mohammadi, and B. Ramavandi, "Elimination performance of methylene blue, methyl violet, and Nile blue from aqueous media using AC/CoFe2O4 as a recyclable magnetic composite," Environmental Science and Pollution Research, vol. 26, pp. 19523-19539, 2019.

[73] M. Malakootian, A. Nasiri, and H. Mahdizadeh, "Metronidazole adsorption on CoFe2O4/activated carbon@chitosan as a new magnetic biocomposite: modelling, analysis, and optimization by response surface methodology," Desalination and Water Treatment, vol. 164, pp. 215-227, 2019.

[74] E. M. Kalhori, T. J. Al-Musawi, E. Ghahramani, H. Kazemian, and M. Zarrabi, "Enhancement of the adsorption capacity of the light-weight expanded clay aggregate surface for the metronidazole antibiotic by coating with MgO nanoparticles: Studies on the kinetic, isotherm, and effects of environmental parameters," Chemosphere, vol. 175, pp. 8-20, 2017.

[75] P. Koohi, A. Rahbar-kelishami, and H. Shayesteh, "Efficient removal of congo red dye using Fe3O4/NiO nanocomposite: Synthesis and characterization," Environmental Technology & Innovation, vol. 23, p. 101559, 2021.

[76] H. F. Alesary, A. H. Odda, H. K. Ismail, W. H. Hassan, G. A. Alghanimi, A. F. Halbus, et al., "Green triiron tetraoxide@Algae (Fe3O4@Algae) nanoparticles for highly efficient removal of lead (Pb2+), cadmium (Cd2+), and aluminum (Al3+) from contaminated water: an isothermal, kinetic, and thermodynamic study," Environmental Science and Pollution Research, vol. 32, pp. 6817-6838, 2025.

[77] A. R. Kul, A. Aldemir, and H. Koyuncu, "An investigation of natural and modified diatomite performance for adsorption of Basic Blue 41: Isotherm, kinetic, and thermodynamic studies," Desalination Water Treat, vol. 229, pp. 384-394, 2021.

[78] M. K. Mohammadi Nodeh, S. Soltani, S. Shahabuddin, H. Rashidi Nodeh, and H. Sereshti, "Equilibrium, Kinetic and Thermodynamic Study of Magnetic Polyaniline/Graphene Oxide Based Nanocomposites for Ciprofloxacin Removal from Water," Journal of Inorganic and Organometallic Polymers and Materials, vol. 28, pp. 1226-1234, 2018.